Journal of
Composites Science

MDPI

Article

Numerical Investigation of the Structural Behavior of an Innovative Offshore Floating Darrieus-Type Wind Turbines with Three-Stage Rotors

Mohamed Amine Dabachi [1,*], Marwane Rouway [2,3], Abdellatif Rahmouni [1], Otmane Bouksour [1], Sara Jamoudi Sbai [3,4], Houda Laaouidi [5], Mostapha Tarfaoui [5,6], Abdelwahed Aamir [7] and Oumnia Lagdani [5]

1 Laboratory of Mechanics Production and Industrial Engineering (LMPGI), High School of Technology (ESTC), Hassan II University of Casablanca, Route d'El Jadida, Km 7, Oasis, Casablanca 8012, Morocco; abd.rahmouni@gmail.com (A.R.); bouksour2@gmail.com (O.B.)
2 LPMAT Laboratory, FSAC, Hassan II University, Casablanca 20100, Morocco; marwanerouway@gmail.com
3 REMTEX Laboratory, ESITH, Casablanca 20000, Morocco; jamoudi.sa@gmail.com
4 LIMAT Laboratory, FSBM, Hassan II University, Casablanca 20000, Morocco
5 IRDL Laboratory, ENSTA Bretagne, UMR-CNRS 6027, 29200 Brest, France; laaouidi.h@gmail.com (H.L.); mostapha.tarfaoui@ensta-bretagne.fr (M.T.); oumnialagdani@gmail.com (O.L.)
6 Green Energy Park (IRESEN/UM6P), Km 2 R206, Benguerir 43150, Morocco
7 MEET Laboratory, FSTS, Hassan I University, BP 577, Settat 26002, Morocco; profaamir2012@gmail.com
* Correspondence: ma.dabachi@ensem.ac.ma; Tel.: +212-645785786

Abstract: The vertical axis wind turbine (VAWT) design has several advantages for offshore wind turbine installation. The VAWT provides omnidirectional wind power, and its mechanical rotating mechanisms can be installed near sea level. In this paper, the selection of a suitable composite material for floating H-Darrieus-type wind turbines with three-stage rotors and its properties are discussed. The centrifugal forces acting on the composite blades are compared to the values of these forces evaluated on the aluminum blades. Abaqus software is used for numerical simulations. The selection of appropriate laminations used to model the composite materials is discussed. The optimum combination of selected layers is determined to reduce the values of maximum bending stresses and displacements, resulting in a high strength-to-weight ratio. In the post-processor, a path is taken at the location of the application of the maximum load on the blade and the values of the displacements and stresses along this path are determined. These maximum values are compared to the unidirectional strength of the selected composite material to ensure a safe design.

Keywords: floating wind turbines; H-Darrieus VAWT; three-stage rotors; finite element; structural analysis

Citation: Dabachi, M.A.; Rouway, M.; Rahmouni, A.; Bouksour, O.; Sbai, S.J.; Laaouidi, H.; Tarfaoui, M.; Aamir, A.; Lagdani, O. Numerical Investigation of the Structural Behavior of an Innovative Offshore Floating Darrieus-Type Wind Turbines with Three-Stage Rotors. *J. Compos. Sci.* **2022**, *6*, 167. https://doi.org/10.3390/jcs6060167

Academic Editor: Francesco Tornabene

Received: 26 March 2022
Accepted: 6 June 2022
Published: 8 June 2022

1. Introduction

Composite materials have played an important role throughout the history of mankind, from housing early civilizations to creating future innovations. Composites offer many advantages such as corrosion resistance, design flexibility, durability, lightness, and strength [1–4]. Composites are present in our daily lives, including products used in construction, medical applications, transportation, sports, aerospace, and the field of marine renewable energy. Modern offshore wind turbine blades are large structures, with complex geometries and various composite material configurations [5–8]. Offshore wind turbines have grown from machines of less than 100 kW to impressive high-technology machines with an output of more than 5 MW and a rotor diameter of up to 126 m. With their increase in size, wind turbines have also become more optimized in terms of structural dimensions and the use of composite materials. These factors complicate the design and the analysis process as the number of design variables are specified by the design requirements of the international IEC 61400-1 specification [9] and the Germanischer-Lloyd regulations [10].

In addition, wind turbine blades are subject to numerous aerodynamic load cases and design constraints which further increase the challenge. The evolution of the rotor and blade design is a balanced integration of economic, aerodynamic, structural, acoustic, and aesthetic considerations that, through experimental testing, have resulted in a three-bladed composite rotor design that meets the needs of the market. For a given strength and stiffness, the blade must be as light as possible to minimize inertial and centrifugal loads which contribute to fatigue. Reducing the values of centrifugal loads is important for a safe blade design, which in turn reduces bending stresses and displacements, and this is the main objective of this study.

Miliket et al. [11] investigated the strength of several factors impacting the aerodynamic performance of H-Darrieus VAWTs. In this work, advanced computational methods were applied to improve the efficiency of self-starting features. For this purpose, a fluid–structure interaction (FSI) was carried out on a 2 kW VAWT to evaluate the structural performance of the two materials widely used for wind turbine blades, which are fiberglass and aluminum alloy. Hand et al. [12] studied the structural analysis of a 5 MW VAWT blade under high wind load in the flapping direction, and used the finite element method of the Ansys workbench software without considering the centrifugal forces which are very important in the structural analysis of VAWT blades. Properties associated with the structural design of the VAWT blade was defined and an overview of the blade response to this load was described. The material and structural characteristics of the VAWT blade were determined by the extreme loading condition. The results show that the blade can withstand this critical load with allowable levels of material deformation, and that the mid-span deflection is less than 3% of the blade span. Rahman et al. [13] studied a V-shaped turbine rotor with three different blade geometries to examine its structural and aerodynamic characteristics. The experimental and numerical data show good accordance with a difference of 15%. According to the static and dynamic study, the results show a better performance for the three-bladed rotor with a 45-degree tilt angle. Elhenawy et al. [14] investigated the effect of F-MWCNTs on the mechanics and deflection of reinforced epoxy composites. The obtained results demonstrate that mixing F-MWCNTs with epoxy resin employing a sonication process has a significant influence on the mechanical properties. A substantial improvement in deflections was determined based on finite element analysis (FEA).

In addition, Tarfaoui et al. [15] investigated the mechanical performance and the structural stability of a large offshore wind turbine blade with critical load conditions using the blade element momentum subroutine in Abaqus. The objective is to evaluate the potential of carbon fiber and glass fiber composite materials, their effect on reducing rotor weight, increasing wear resistance, and their stiffness. Similarly, Tarfaoui et al. [16,17] performed a finite element modal analysis of full-scale 48 m fiberglass composite blades with a 5 MW blade using Abaqus. The overall blade can benefit from weight reduction due to the decrease in dynamic loads. Numerical analysis was performed to find the most suitable spar geometry and to understand the complex structural design behavior of the blades. There are five different types of structural strengthening that avoid undesirable structural mechanisms.

Li et al. [18] studied the structural performance of a solid aluminum VAWT blade. In a similar study, Marsh et al. [19] compared the structural performance of straight-blade and bladed helical VAWTs using a fluid–structure interaction approach. However, the VAWT structure, including its blades, were assumed to be completely made from steel and it is unknown how practical this material and design selection would be. However, early research at Sandia National Laboratories (SNL) showed that metallic materials should be avoided for the structural design of VAWTs due to blade mass and fatigue strength issues [20–22].

The purpose of this paper was to study the durability of Darrieus-type floating wind turbine blades with three-stage rotors under extreme load conditions [23,24]. Considering the applied stresses, perfect long-term durability is required. FEM allows the selection of materials (fiber, matrix), fiber architectures (plies, tissues), and the optimization of lay-up

sequences that minimize the sensitivity to mechanical stresses applied to the structures. The rest of the paper is organized as follows: floating Darrieus-type wind turbine with three-stage rotors is discussed in Section 2. Section 3 is devoted to the materials and methods. Section 4 presents the first case study of rotor blade 1 made of an isotropic material to find the optimal value of the thickness, while Section 5 presents the results and discussion of the blades of the three composite rotors. Lastly, Section 6 concludes the paper.

2. Floating Darrieus-Type Wind Turbine with Three-Stage Rotors

In previous work [24], the conceptual design of floating Darrieus-type wind turbines with three-stage rotors were outlined. The rotors will be designed with a straight-blade configuration, because it has been demonstrated to have the best aerodynamic performance and self-regulation at all wind velocities over other possible configurations [24]. The design provides a higher height to benefit from the highest winds. The three rotors of the turbine rotate about the fixed shaft independently, in contrast to traditional VAWTs where both a rotor and a shaft rotate at the same time, which leads to the increase in inertia and the applied torque to the shaft and creates problems for the self-starting of the turbine. Figure 1 shows the 3D design of Darrieus-type floating wind turbines with three-stage rotors under extreme wind loading on each blade.

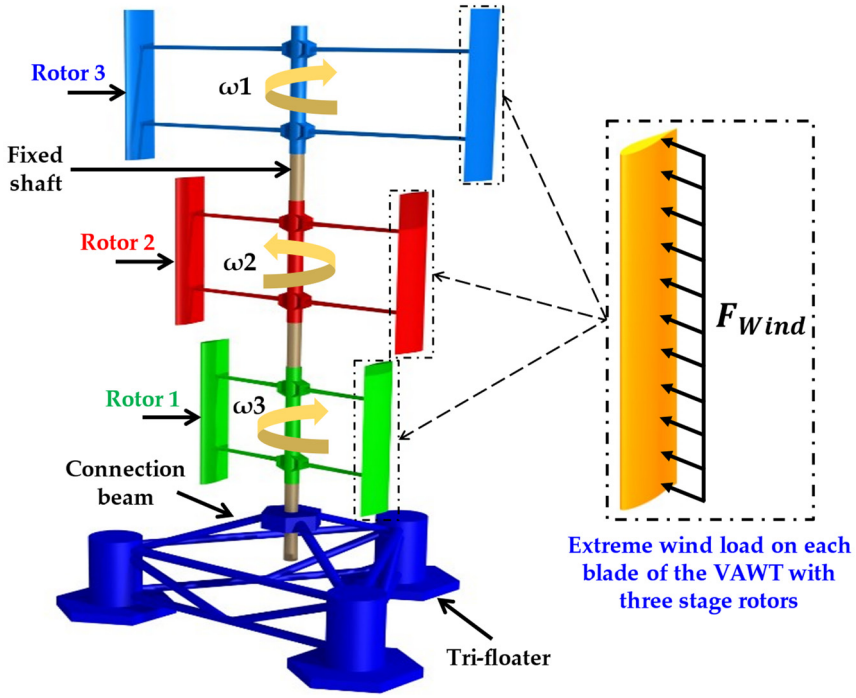

Figure 1. Three-dimensional design of a Darrieus-type floating wind turbine with three-stage rotors under extreme wind load on each blade.

3. Materials and Methods

3.1. Abaqus Code

In this quest for increasingly efficient computer-aided design and calculation software, we can mention the Abaqus software. The Abaqus code is a famous software for the finite element (FE) simulation of various problems in continuum mechanics. It is very widespread and well known, particularly for its efficient treatment of non-linear problems [25]. Abaqus is widely used in the automotive, aeronautics, as well as in the marine renewable energy industries [26]. Due to its wide range of analysis capabilities and good usability, it is also very popular in academia for scientific research. As presented previously, an F-VAWT is a complex composite structure. Therefore, the study of the impact of the maximum stresses and maximum strains of such a structure represents a great difficulty. Figure 2a,b present an explanatory diagram of the passage from a continuous model to a discrete model. In any

numerical modeling, we need inputs that allow us to describe the behavior of the structure. These can be of different origins: geometry, materials, boundary conditions, loads, etc.

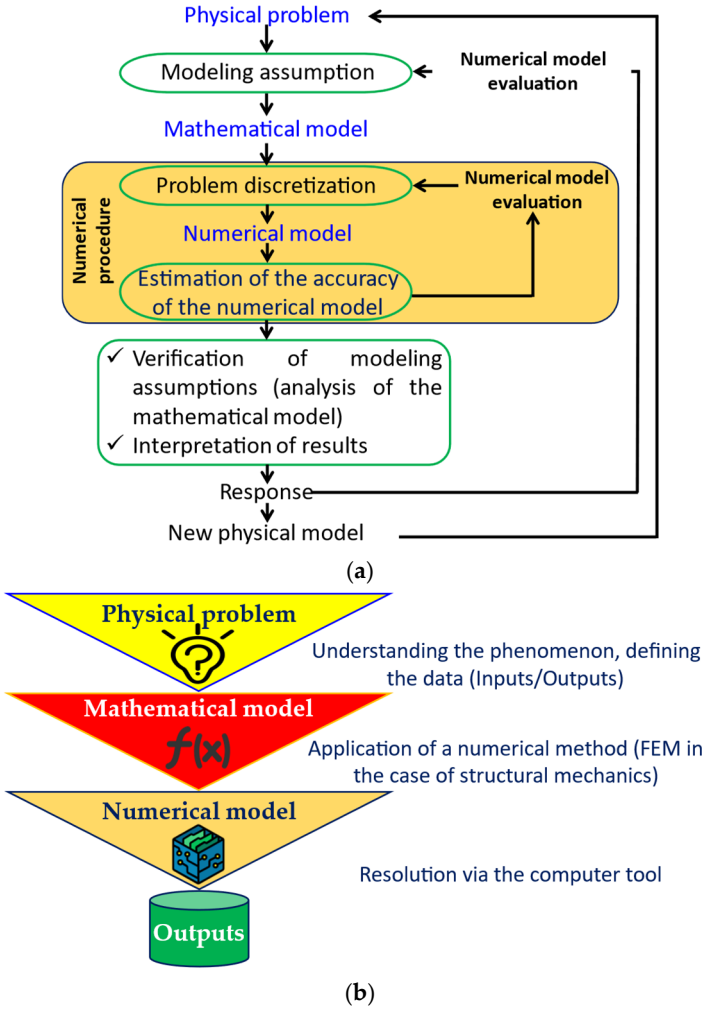

Figure 2. (**a**) Explanatory diagram of the transition from a continuous to a discrete model; and (**b**) approach to solving complicated physical problems.

3.2. Validation of Abaqus Code

In order to show the validity of this code, Abaqus was compared with the research results of Saqib et al. [27] in terms of the maximum values of the strains of different thickness values of a straight VAWT blade. The authors [27] used beam theory for analytical modeling and ANSYS 11.0 code for numerical simulation. However, before launching the validation, it is essential to perform a mesh convergence study.

3.2.1. Selecting the Type of Mesh Element

We chose a solid (continuous) three-dimensional C3D8R hexahedral type element because it generally provides an equivalent accuracy solution at a lower cost. C3D8R is a general-purpose linear brick element with 8 nodes and reduced integration (1 integration point). The shape functions are the same as for the C3D8R element and can be found in [28]. The integration point is shown in Figure 3. The obtained optimal element size will then be applied in the next section for our modeling cases. Reasons for choosing the C3D8R element include the fact that the solid elements reflect the 3D reality of the physical model.

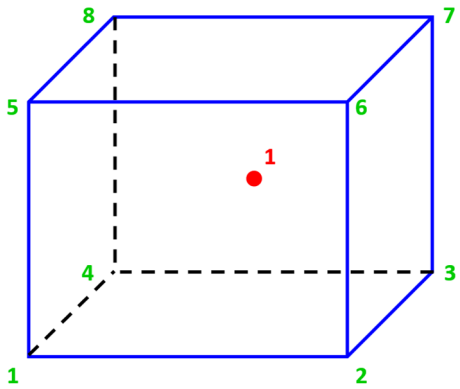

Figure 3. Representation of the 1 × 1 × 1 integration points scheme in hexahedral elements.

3.2.2. Mesh Convergence Study

To define an optimal mesh size to reduce the computation time without altering the numerical solution, we used a sensitivity study. The evolution of the maximum values of the deformations as a function of the size of the element is represented in Figures 4 and 5. The results of the successive calculations seem to converge from 46,000 elements, which correspond to a mesh size of 7 mm.

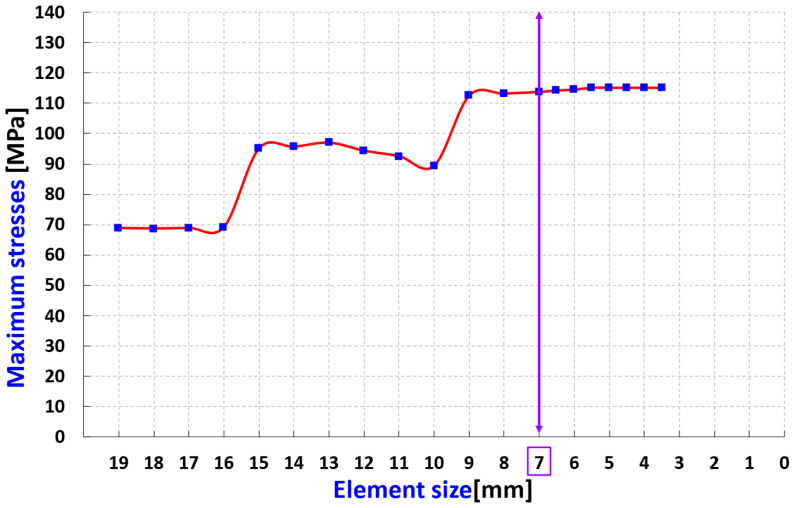

Figure 4. Mesh convergence study—maximum constraints as a function of element size.

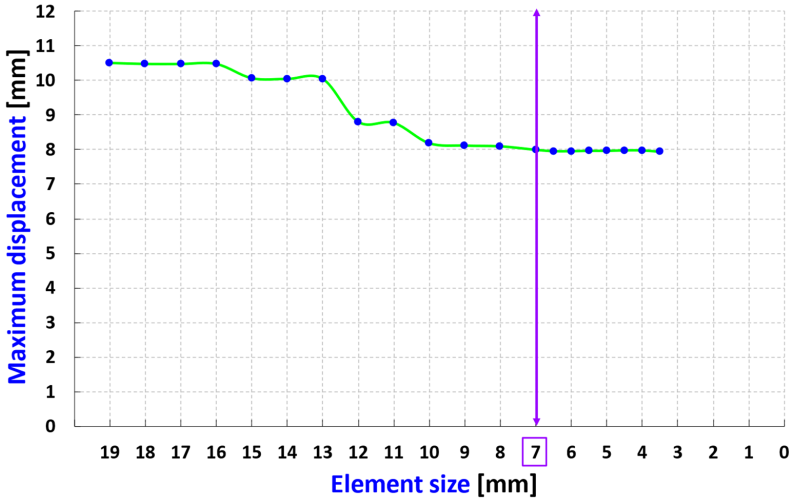

Figure 5. Mesh convergence study—maximum displacement as a function of element size.

Considering the strong evolution of the CPU as a function of the number of elements, it is unnecessary to refine the mesh as further refinement of the mesh does not change the final results of the numerical analysis.

The comparison of the maximum displacements with the analytical and numerical results is presented in Figure 6 and Table 1. It can be observed that the simulation results of the Abaqus code show good agreement with the analytical and numerical results of the Ansys code with an acceptable relative error for the different values of the blade thickness.

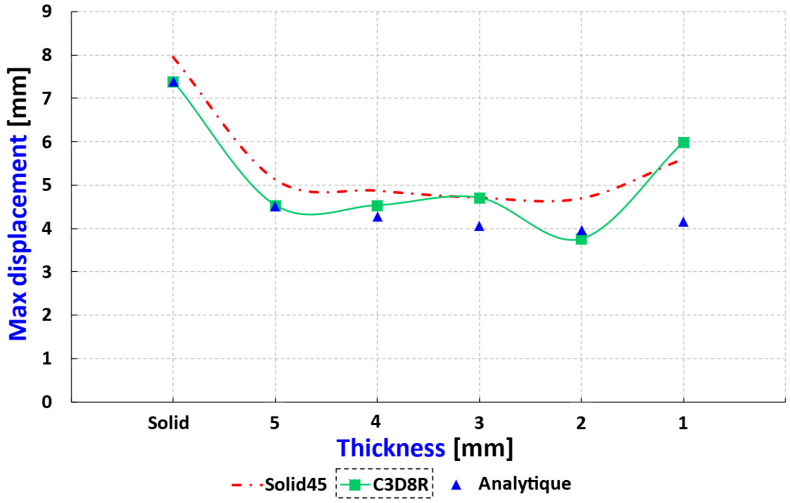

Figure 6. Comparison of maximum displacement with analytical and numerical results of saqib et al. [27].

Table 1. Comparison of maximum displacements as a function of different thickness values from analytics, Ansys, Abaqus, and their relative errors.

Thickness (mm)	Max. Displacement (mm)			Error % Compared to Analytical	
	Solid45 Ansys [27]	C3D8R Abaqus	Analytical [27]	Solid45 Ansys [27]	C3D8R Abaqus
Solid	7.947	7.392	7.39	7.54	0.03
5	5.123	4.532	4.51	13.59	0.48
4	4.864	4.532	4.27	13.91	5.95
3	4.703	4.705	4.07	15.55	14.47
2	4.689	3.756	3.97	18.11	5.6
1	5.603	5.989	4.17	34.36	35.81

This research work is the continuation of our first work published in 2019 [24]: the purpose of this paper will be to study the durability of Darrieus-type floating wind turbine blades with three-stage rotors under extreme load conditions [23,24]. Considering the applied stresses, perfect long-term durability is required. FEM allows the selection of materials (fiber, matrix), fiber architectures (plies, tissues), and the optimization of lay-up sequences that minimize the sensitivity to mechanical stresses applied to the structures. We used the macros function of Excel in coupling with Catia and Abaqus for the analysis and structural optimization of the 3 rotors of our design. Figure 7 outlines the step-by-step procedure for the structural analysis of composite blades of vertical axis wind turbines with three-stage rotors.

3.3. Geometry and Boundary Conditions

The two inserts representing the two blade supports are placed between 21% and 79% along the length of the blade (see Figure 8). For symmetrical airfoils, the center of pressure and the aerodynamic center are located at the quarter chord (c/4) of the leading edge [29]; at this position, the total force (normal aerodynamic force + centrifugal force) must be applied in perpendicular to the blade chord. The normal aerodynamic force applied to the

blade was previously calculated, but the centrifugal force remains to be calculated, as we will see in the following sections.

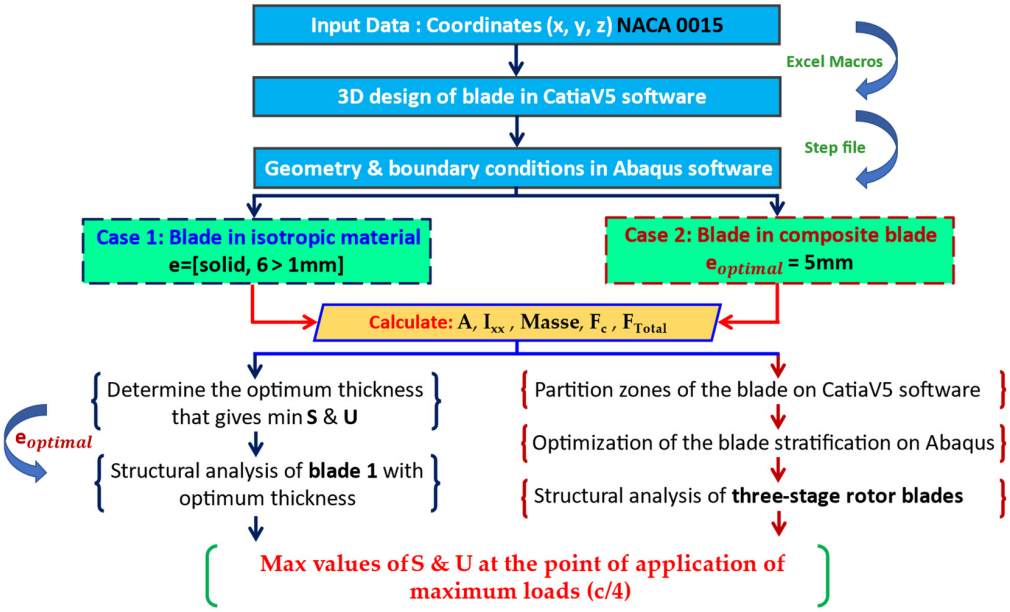

Figure 7. General approach to the structural analysis of composite blades of vertical axis wind turbines with three-stage rotors.

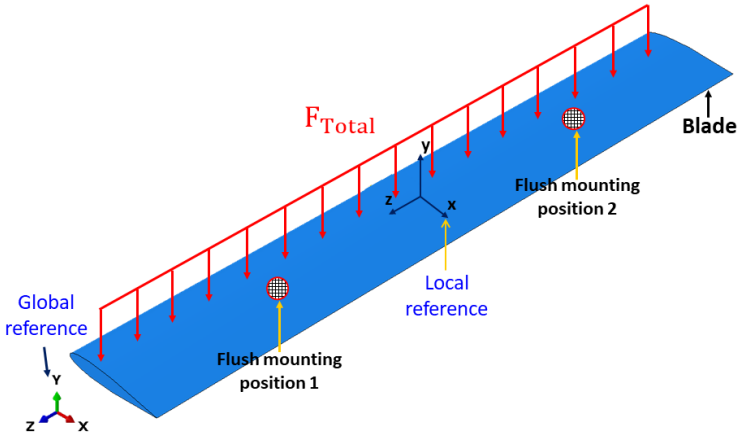

Figure 8. Illustration of the total load on the VAWT blade along the length of the blade.

Thickness-to-chord ratio for NACA 0015 airfoil

For a symmetrical four-digit NACA profile, the thickness-to-chord ratio is given by the following equation [30]:

$$\pm\frac{z}{c}=\frac{t}{0.2}\left[0.2969\sqrt{\frac{x}{c}}-0.126\left(\frac{x}{c}\right)-0.3516\left(\frac{x}{c}\right)^2+0.2834\left(\frac{x}{c}\right)^3-0.1015\left(\frac{x}{c}\right)^4\right] \quad (1)$$

where t is the maximum thickness of the section as a fraction of the chord size.

Surface of the aerodynamic profile

$$A=\int_0^c\left[\left(+\frac{z}{c}\right)-\left(-\frac{z}{c}\right)\right]dx \quad (2)$$

Moment of inertia

$$I_{xx}=\int_0^c\frac{1}{3}\left[\left(+\frac{z}{c}\right)^3-\left(-\frac{z}{c}\right)^3\right]dx \quad (3)$$

4. Case 1: Blade in Isotropic Material

In this first case, the F-VAWT three-stage rotor 1 blade model was optimized from a solid cross-section to a hollow cross-section with different thickness values to reduce the weight and centrifugal forces on the blade. The cross-sectional properties can be calculated using relations (1)–(3) or with the beam section properties function of Catia V5. Figure 9 shows the different thickness values of the cross-sections of rotor blade 1.

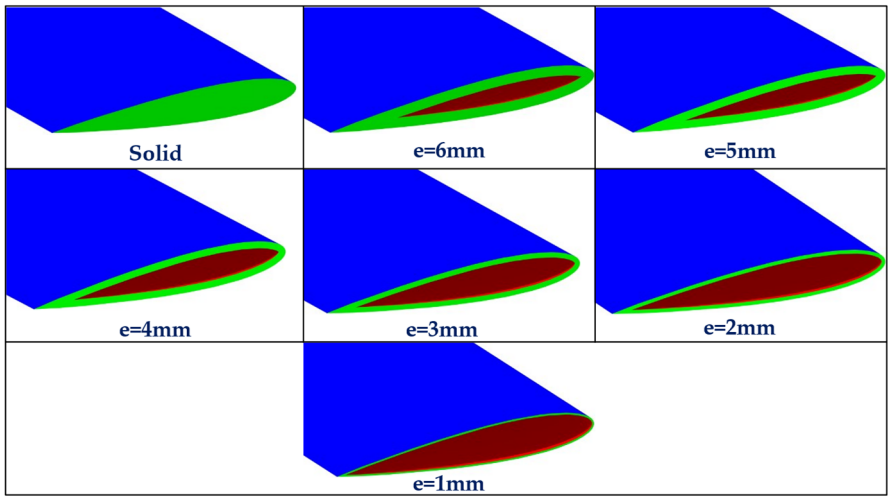

Figure 9. Cross-sections of the designed models of the rotor blade 1 with different thickness values.

4.1. Selection of the Appropriate Isotropic Material

Aluminum is a more used material for VAWT wind turbines, especially for domestic wind turbines. Therefore, we chose this material to optimize the blade and find the optimal thickness that will later help us optimize the composite blade in terms of lamination and the optimal number of plies. The blade is designed in aluminum EN AW-2017 [31], and its characteristics are presented in Table 2.

Table 2. Mechanical properties of aluminum EN AW-2017.

Properties	Yield Strength (MPa)	Breaking Strength (MPa)	Young's Modulus (GPa)	Poisson's Ratio (-)	Density (kg/m^3)
Values	295	470	70	0.346	2710

4.2. Analytical Calculation of Centrifugal and Total Forces

The high values of centrifugal forces play an important role in the design of the straight blades of a vertical axis wind turbine. Centrifugal forces add to the aerodynamic forces and lead to high values of bending stresses and displacements in these blades. The straight blades with a high aspect ratio of the H-Darrieus rotor are subjected to high values of centrifugal forces, values which are determined for different values of the blade thickness of rotor 1 (with mass m) at the maximum speed $R\omega$ which is equal to 42.60 m/s using the following equation [27]:

$$F_c = \frac{2mR\omega^2}{D} \quad (4)$$

where D is the diameter of the rotor.

Table 3 gives the values of the centrifugal and total forces for different blade thicknesses of rotor 1. The total force evaluated here is the sum of the centrifugal force determined at the maximum tip speed and the extreme aerodynamic force perpendicular to the chord, 314 N.

Table 3. Value of the centrifugal and total forces for different thicknesses of rotor blade 1.

Rotor 1					
Thickness (mm)	**A (m^2) (10^{-3})**	**I_{xx} (m^2) (10^{-3})**	**Masse (kg)**	**F_c (KN)**	**F_{Total} (KN)**
Solid	2.000	6.733	6.262	11.364	11.678
6	2.000	6.271	4.276	7.759	8.703
5	1.000	5.880	3.679	6.676	6.990
4	1.000	5.297	3.033	5.504	5.818
3	0.863	4.472	2.339	4.244	4.558
2	0.590	3.352	1.600	2.903	3.217
1	0.302	1.881	0.819	1.486	1.800

4.3. Results and Discussion

- The values of the maximum stresses and displacements decrease from the solid section to the hollow section up to a blade thickness of approximately 5 mm, but increase with a further reduction in the value of the blade thickness (see Figures 10–12 and Table 4).

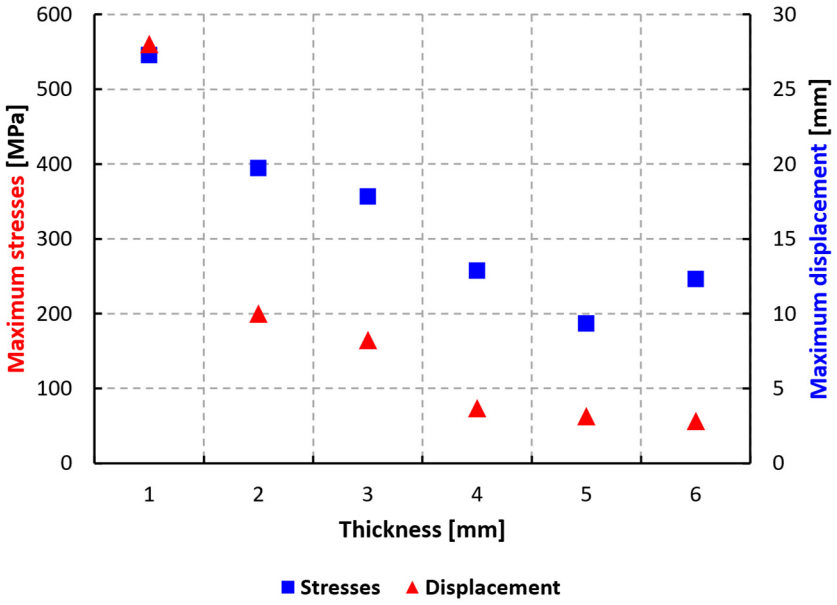

Figure 10. Displacement curves and maximum stresses for different values of rotor blade thickness 1.

Table 4. Displacements and maximum stresses for different values of the thickness and mass of the rotor blade 1.

Thickness (mm)	Mass (kg)	Max Stresses (MPa)	Max Displacements (mm)
Solid	6.262	193.979	4.489
6	4.276	246.004	2.843
5	3.679	186.581	3.150
4	3.033	257.295	3.674
3	2.339	356.270	8.246
2	1.600	394.573	9.996
1	0.819	545.851	28.032

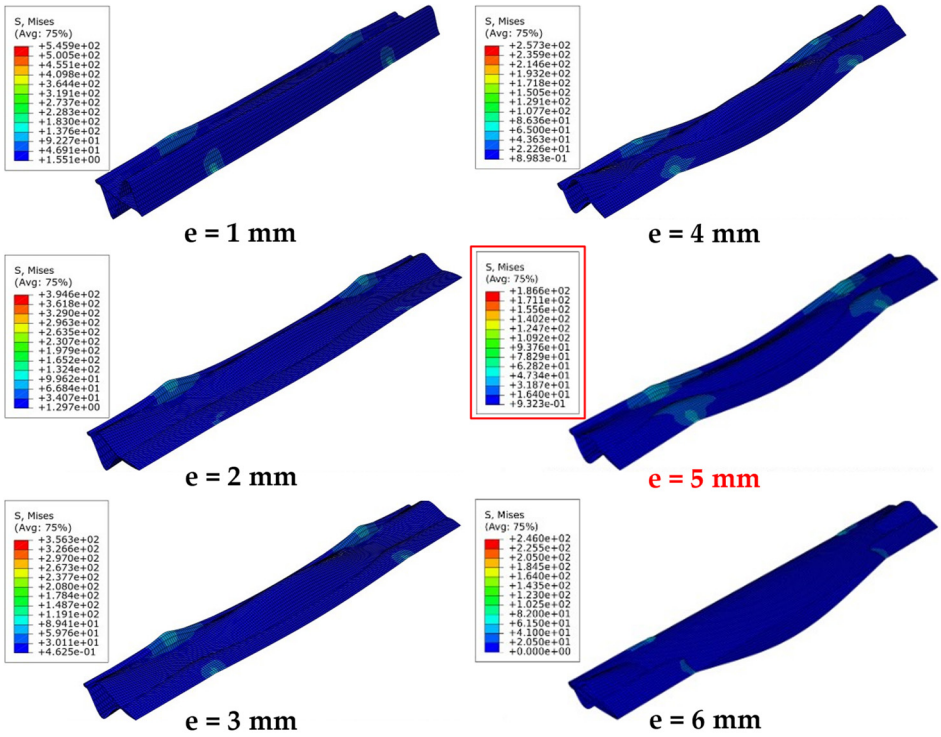

Figure 11. Plot of the quarter chord trajectory along the length of the VAWT blade span.

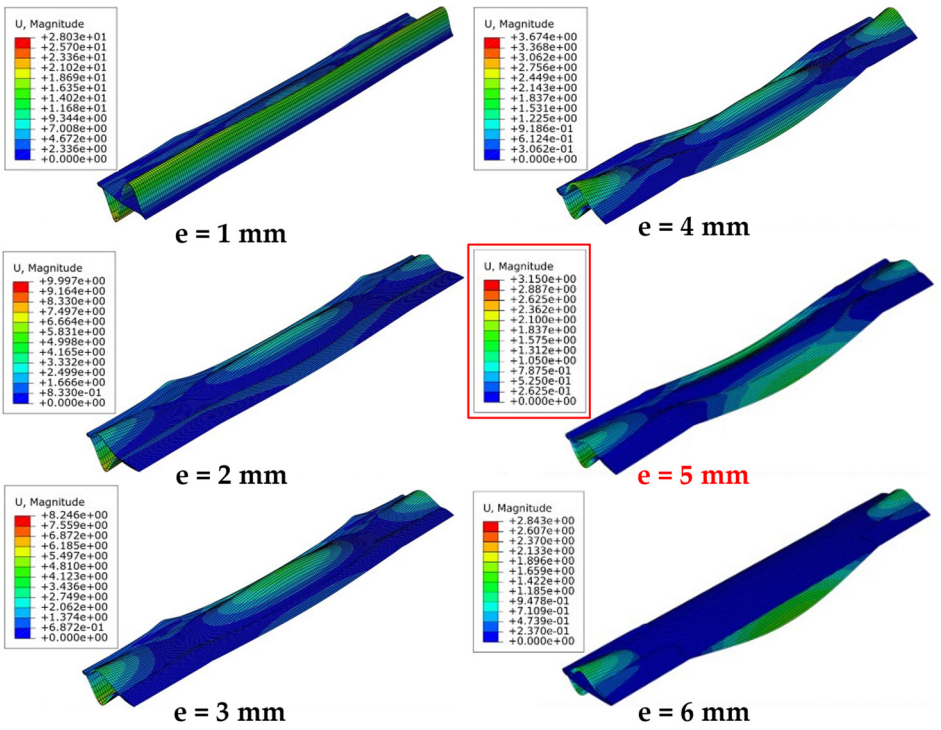

Figure 12. Displacement U for different thickness values of Aluminum 1 rotor blade after the application of extreme loads.

- When the cross-sections of these blades were modeled and analyzed, it was observed that the distortion of the blade shape occurs in the regions of maximum deformations, as shown in Figure 13.

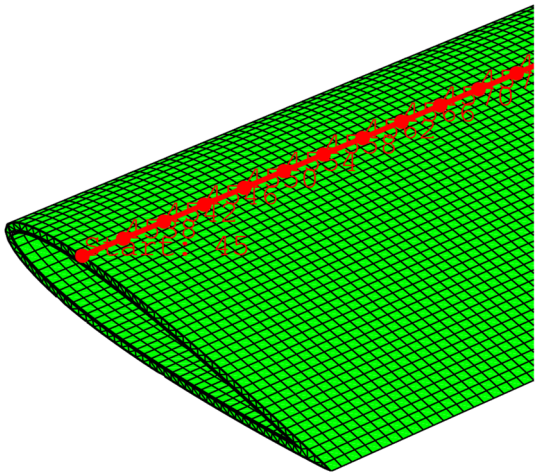

Figure 13. Von Mises stresses S for different thickness values of aluminum rotor 1 blade after the application of extreme loads.

- The values of the maximum displacements and stresses suddenly increase from 4 to 1 mm thickness. This is due to the large deformation of the blade shape. The C3D8R element type gives a better approximation of the large deformation of the blade shape.
- The distortion of the blade shape decreases with increasing thickness.
- The optimum value for the thickness of rotor blade 1 is 5 mm because this value considerably reduces the maximum stresses and displacements applied to the blade, as well as reducing their weight. In the case of using an orthotropic material, this optimal thickness value will be used.
- A plot is considered by selecting all nodes along the quarter chord (see Figure 12).
- As shown in Figure 14, the maximum values of the stress variation and displacements of rotor blade 1 of an optimum thickness of 5 mm are evaluated at the point of the application of maximum loads (c/4) along the length of the blade.

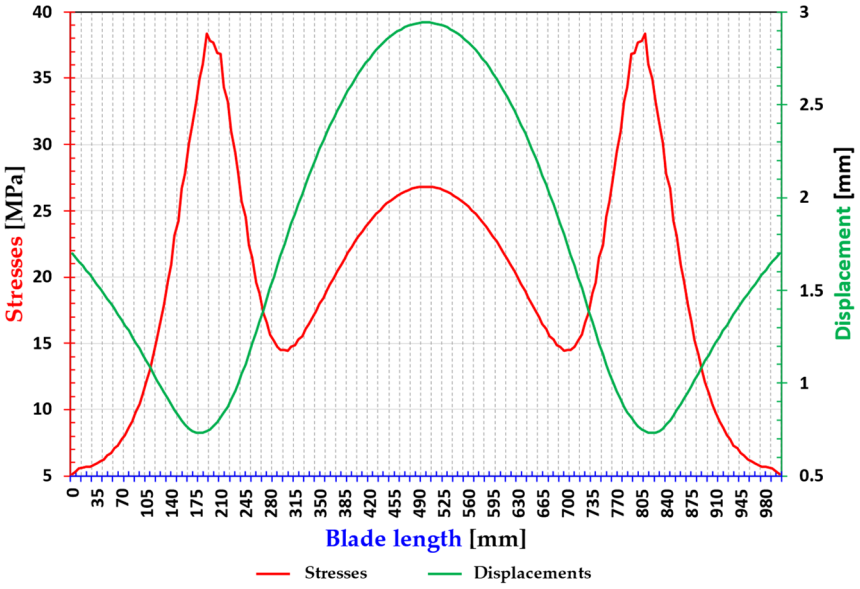

Figure 14. Maximum values of stresses and displacements at the point of application of the maximum loads (c/4) of the blade of rotor 1 in aluminum with the optimal thickness of 5 mm.

- The maximum stresses are located at positions 200 and 900 mm of the blade length; therefore, the maximum displacements are in the middle of the blade at the position of 625 mm.

- The yield strength of aluminum EN AW-2017 is in the range of 295 MPa (see Table 2) and according to Figure 11 of stress distribution, the Max stress is approximately 186.581 MPa, does not exceed the yield strength of the material, and thus the blade operates in the elastic range which allows it to withstand the extreme loads applied without suffering from cracking or breaking.
- The maximum displacement is approximately 3.150 mm, which is low compared to the dimension of the blade.

5. Case 2: Composite Blade

Centrifugal forces can be reduced by decreasing the weight of the blade which can be achieved by choosing a low-density material. The composite material blade can have thin walls due to the high strength-to-weight ratio of the materials. A straight aluminum VAWT blade was designed in the previous section. The same blade of optimal thickness of 5 mm of rotor 1 is modeled with composite material to optimize its design, i.e., find the optimal thickness of the plies; then, the same process will be applied to the blades of rotors 2 and 3 of our wind turbines.

5.1. Selection of the Appropriate Composite Material

Dynamic stresses and various loading conditions are more severe on straight-blade VAWT than in many other mechanical applications. In order to deliver mechanical or electrical energy according to the operational parameters and surrounding conditions, the typical material of a straight-blade VAWT must have certain useful properties [32]. The most important of these properties are sufficiently high yield strength for a longer service life, high material stiffness to maintain optimal aerodynamic performance, and low density to reduce the gravitational and normal force component. Modern wind turbine materials are composites consisting of fiberglass reinforcements. For turbine blade design, they are composed of fiberglass (E-glass) with epoxy, polyester, or vinyl esters, and normally hand layup manufacturing techniques are used [12,33]. As reported by [34,35], the glass–epoxy composite material is recommended for the design of wind turbine blades because of their useful characteristics. In addition, it is considered as one of the potential materials for the construction of VAWTs with straight blades, because they are economically attractive and have a good combination of material properties (high strength, moderate density, and stiffness). For all these reasons, glass–epoxy was chosen for the straight-blade F-VAWT with three-stage rotors. The properties of glass–epoxy are presented in Table 5 [36]. The density of glass epoxy with V_f = 60% and V_m = 40% is calculated as follows:

$$\rho_c = \rho_f V_f + \rho_m V_m = 2500(0.6) + 1200(0.4) = 1980 \text{ Kg} \cdot \text{m}^{-3} \quad (5)$$

where ρ and V represent the density and volume fraction, respectively. Subscripts f and m denote the fiber and matrix, respectively.

Table 5. Material properties of glass–epoxy layers with fiber volume fraction of 60% and thickness = 0.13 mm.

E_x [MPa]	$E_y = E_z$ [MPa]	$\nu_{xy} = \nu_{xz}$	ν_{yz}	$G_{xy} = G_{xz}$ [MPa]	G_{yz} [MPa]
45×10^3	12×10^3	0.3	0.2	4.5×10^3	5×10^3

5.2. Comparative Study of Aluminum and Glass–Epoxy

The centrifugal and total forces are evaluated again on the same rotor blade 1 using a glass–epoxy composite material. The glass–epoxy material has a lower density than aluminum, which results in a significant reduction in the centrifugal forces acting on the blade. The comparison of the total forces acting on the aluminum and glass–epoxy blades is presented in Table 6. The cross-sectional area of the blade does not change, as it is the total force acting on the blade that changes. The aerodynamic force values remain the

same in both cases since there is no change in the overall aerodynamic shape of the blades. Therefore, the reduction in total forces in the glass–epoxy case is only due to the reduction in centrifugal forces.

Table 6. Comparison of total forces acting on rotor blade 1 for aluminum and glass–epoxy materials as a function of different thicknesses.

Rotor 1								
e (mm)	**A (m^2) (10^{-3})**	**I_{xx} (m^2) (10^{-8})**	**Mass (kg)**		**F_c (KN)**		**F_{Total} (KN)**	
			Al	**V-Epoxy**	**Al**	**V-Epoxy**	**Al**	**V-Epoxy**
6	2.000	6.271	4.276	3.124	7.759	5.669	8.703	5.983
5	1.000	5.880	3.679	2.688	6.676	4.878	6.990	5.192
4	1.000	5.297	3.033	2.216	5.504	4.021	5.818	4.335
3	0.863	4.472	2.339	1.709	4.244	3.101	4.558	3.415
2	0.590	3.352	1.600	1.169	2.903	2.121	3.217	2.435
1	0.302	1.881	0.819	0.598	1.486	1.085	1.800	1.399

5.3. Calculation of Centrifugal and Total Forces

Table 7 summarizes the values of centrifugal and total forces acting on the composite blade for the three H-Darrieus floating wind turbine rotors.

Table 7. Total forces acting on the composite blade for three rotors.

$e_{optimal}$ = 5 mm					
Rotors	**A (10^{-3}) (m^2)**	**I_{xx} (10^{-3}) (m^2)**	**Mass (kg)**	**F_c (kN)**	**F_{Total} (kN)**
1	1	5.88	2.688	4.878	5.192
2	2	24.18	7.630	8.179	8.997
3	3	63.24	18.501	14.874	16.814

5.4. Zones of Partition and Stratification of the Blade

In order to assign the composite material to each zone of the thickness of the blade, this one was partitioned thanks to the use of the command Macros of Excel, wireframe and surface design, and geometrical bodies via the software Catia V5. This partition allowed to multiply the combinations (i.e., the thickness and orientation of the successive layers) of materials according to the needs. These partitions are illustrated in Figure 15. Figure 16 represents the stratification of the blade with images from the Abaqus finite element software.

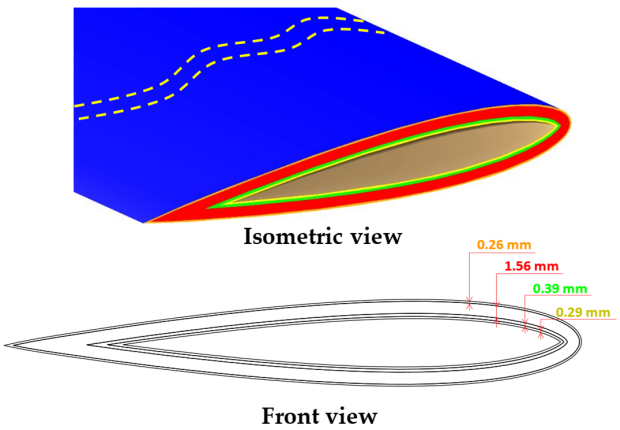

Figure 15. Illustration of the partition zones of the blade.

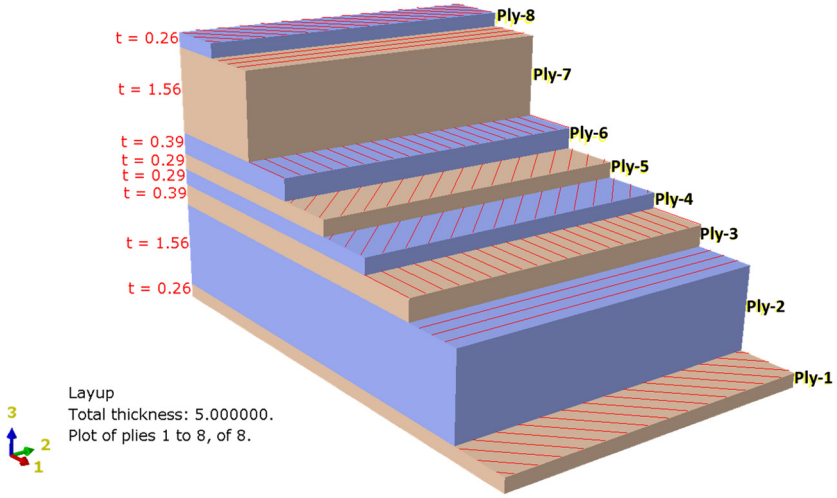

Figure 16. Illustration of the stratification of the blade on Abaqus.

5.5. Results

5.5.1. Optimization of Laminates

The optimal design of laminates is still a topic of study. In fact, composites and laminates are generally complex and complicated materials whilst their design requires that many parameters be determined and different objectives be reconciled, sometimes in contrast with each other. Designers and scientific researchers must therefore make many choices, and having a simple experiment is sometimes not enough. Our goal is to obtain lower stress and displacement values for glass–epoxy blades than for aluminum blades. Therefore, an appropriate stacking sequence must be chosen to obtain the best results for both stress and displacement (as shown in Table 8 and Figure 17). In the literature [34–37], wind turbine manufacturers have proposed some useful combinations for glass–epoxy layers based on experimental data. A combination of glass–epoxy layers [45°/90°/0°/−45°]s is applied to our blade model, as shown in Figure 15 and recommended by Walczyk [38].

Table 8. Different combinations of glass–epoxy laminates and comparison of results with aluminum (S_{max} = 186.581 MPa, U_{max} = 3.150 mm).

Sequences of Stacking	Thickness of Each Laminate (m)	Stresses Max (MPa)	Displacements Max (mm)
A [45°/90°/0°/−45°]s	0.0005	139	2.010
B [45°/90°/0°/−45°]s	45°: 0.0005 90°: 0.001 0°: 0.0005 −45°: 0.0005	109	2.280
C [45°/90°/0°/−45°/−90°]s	45°: 0.00025 90°: 0.00075 0°: 0.0005 −45°: 0.00075 −90°: 0.00025	132	2.107
D [45°/90°/0°/−45°]s	45°: 0.00026 90°: 0.00156 0°: 0.00039 −45°: 0.00029	102.8	2.335
E [45°/90°/0°/−45°/−90°]s	45°: 0.00026 90°: 0.00078 0°: 0.00042 −45°: 0.00026 −90°: 0.00078	129	2.144

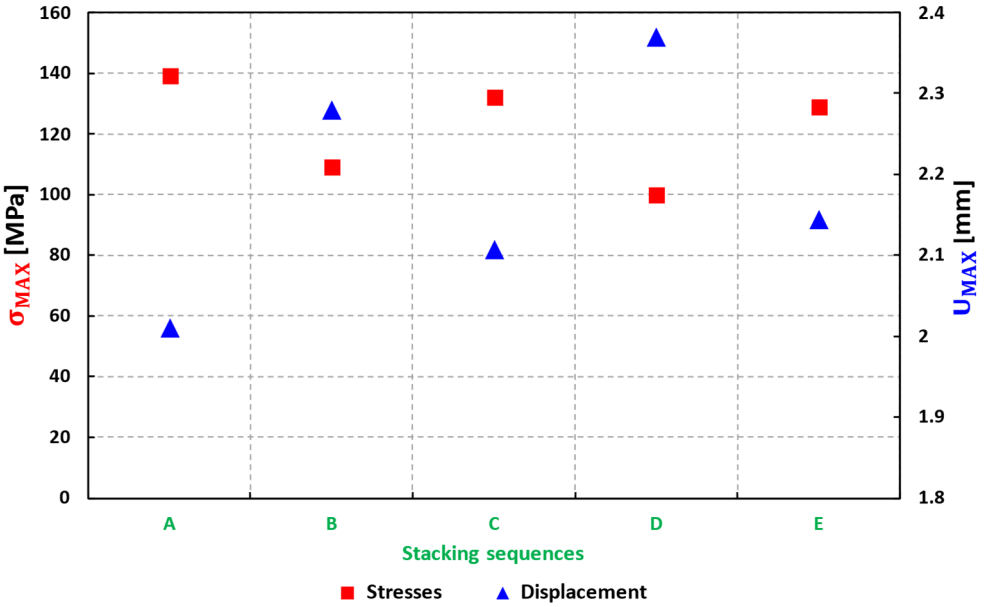

Figure 17. Maximum stresses and displacement curves for different stacking sequences.

The combination of layers in this orientation is first applied with the same thickness, and then the thickness of each layer is varied. Several ply sequences were tested. We present here just a few for information. It can be seen from the results (see Table 8 and Figure 17) that we finally obtained a combination of layers that reduced the values of maximum stresses and displacements compared to aluminum. Table 9 shows the optimal thicknesses of the glass–epoxy plies with their orientation.

Table 9. Optimal thicknesses of the glass–epoxy plies with their orientation.

Layer Number	1	2	3	4	5	6	7	8
Orientation (°)	45	90	0	−45	−45	0	90	45
Thickness (mm)	0.26	1.56	0.39	0.29	0.29	0.39	1.56	0.26
Total Thickness (mm)	5							

The results presented in Figures 17 and 18 show that we finally obtained a combination of layers that reduced the values of maximum stresses and maximum displacements compared to aluminum of the rotor blade 1. The orientation of the glass–epoxy layers [45°/90°/0°/45°]s with variation in the thickness of each layer (as shown in Tables 8 and 9, this was chosen for the best design of the straight blade of a VAWT. For the structural analysis of rotors 2 and 3 of H-Darrieus-type floating wind turbine with three-stage rotors (see Figures 19 and 20), we will use the same optimal thicknesses of glass–epoxy layers with their orientations. Therefore, it can be concluded that the stresses and displacements were also reduced because there are 74% of the total layers facing the load in the 90° direction. At the same time, there are layers in the 0° and 45° orientations that required a reduction in the delamination phenomenon in the composites [39].

5.5.2. Stresses and Displacements of the Composite Blades of Three Rotors

Unidirectional Strength Test

Composite materials are orthotropic materials with distinct properties in different directions. At this point, it is also important to verify that the maximum value of stresses in each direction is not greater than the unidirectional strength of the epoxy glass. The maximum stress values are required at the quarter chord position where the maximum loads on the blade are applied. The variation in the stress and displacement values for the blades of the three rotors along the path is shown in Figures 21–23, respectively. It

can be seen from the three graphs that the maximum stress values for the blades of the three rotors appear at the locations where the blade is embedded; on the other hand, the displacements are minimal at the same location and the maximum displacements are in the middle of the blade. The maximum stress values in the x (S_x) and y (S_y) directions along the path for the blades of the three rotors are compared to the unidirectional strength of the epoxy glass in each direction. As shown in Table 10, the comparison shows that the maximum stress values—obtained for this design for the blades of the three rotors—are less than the maximum allowable unidirectional stresses for the glass–epoxy composite material. Therefore, the design of this blade is safe.

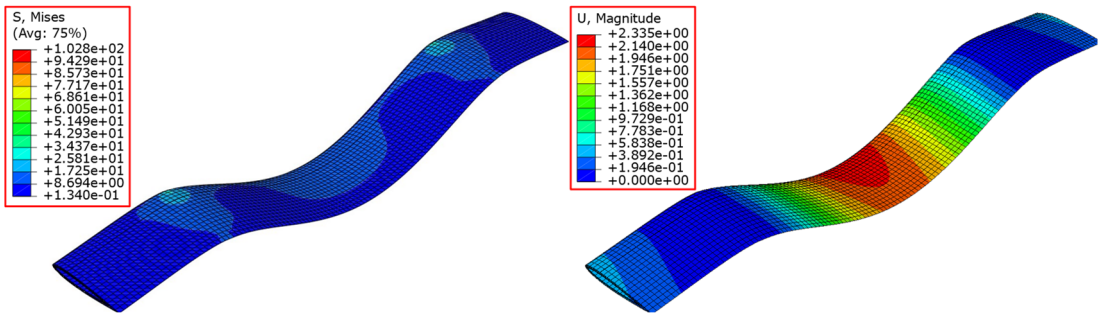

Figure 18. Von Mises stress S and displacements U with the optimal thickness of 5 mm of the rotor blade 1 in V-Epoxy after the application of extreme loads.

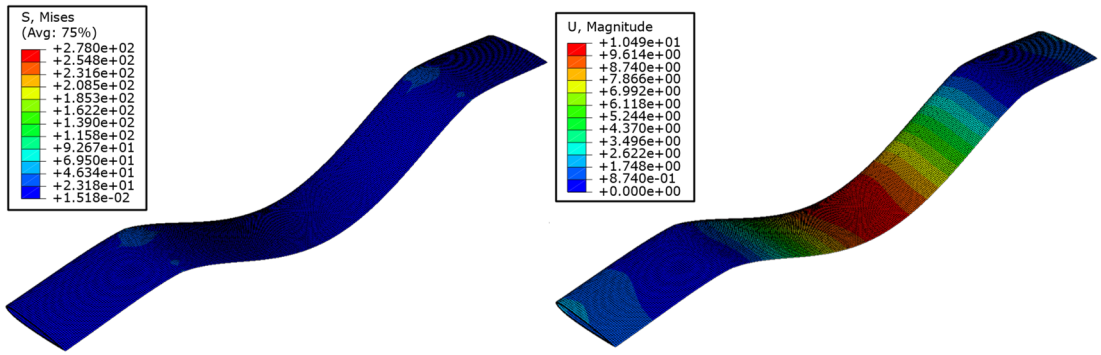

Figure 19. Von Mises stress S and displacements U with the optimal thickness of 5 mm of the V-Epoxy rotor blade 2 after the application of extreme loads.

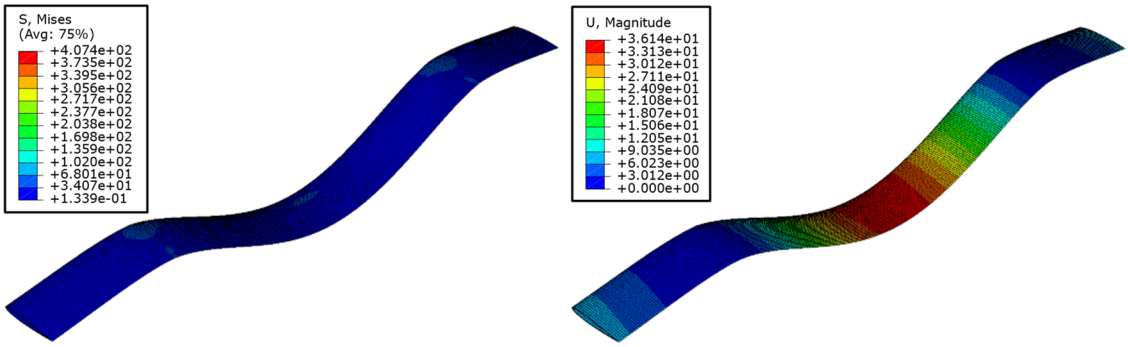

Figure 20. Von Mises stress S and displacements U with the optimal thickness of 5 mm of rotor blade 3 in V-Epoxy after applying extreme loads.

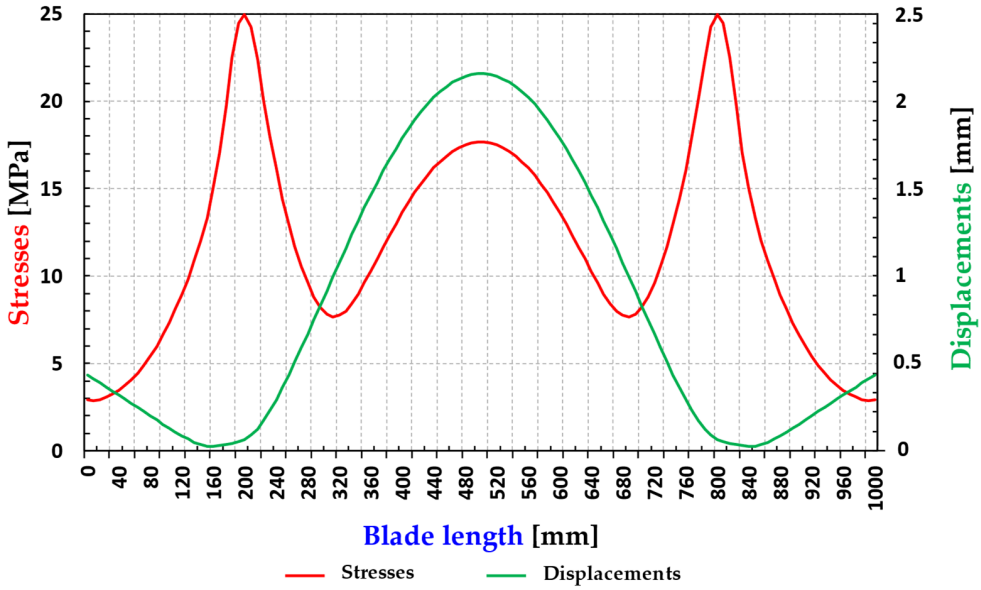

Figure 21. Maximum values of the stresses and displacements at the point of application of maximum loads (c/4) of rotor blade 1 made of V-Epoxy with the optimum thickness of 5 mm.

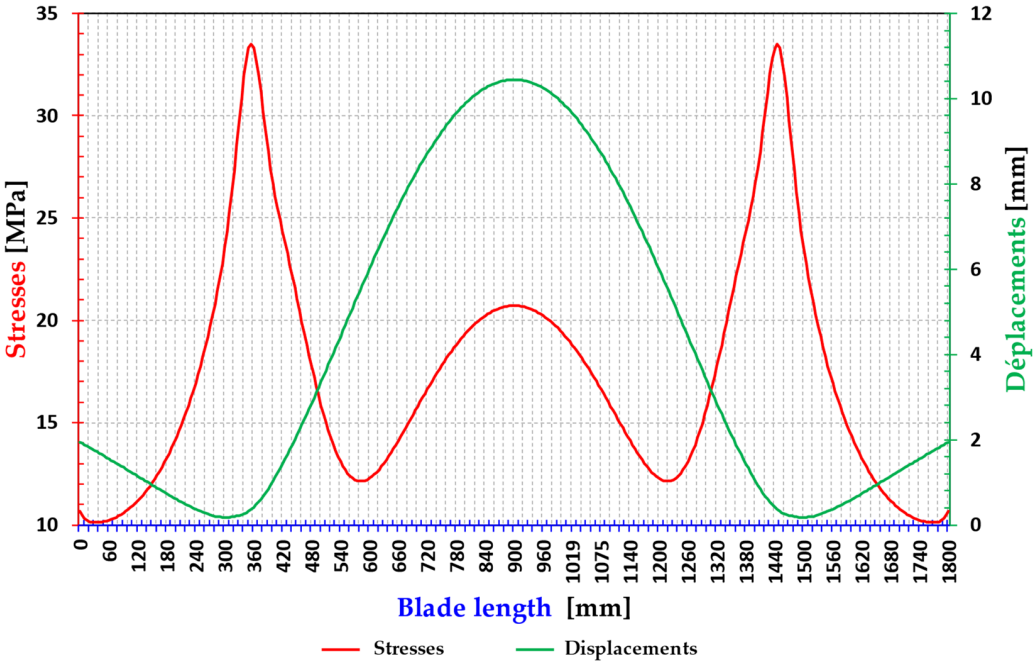

Figure 22. Maximum values of stresses and displacements at the point of application of maximum loads (c/4) of rotor blade 2 made of V-Epoxy with the optimal thickness of 5 mm.

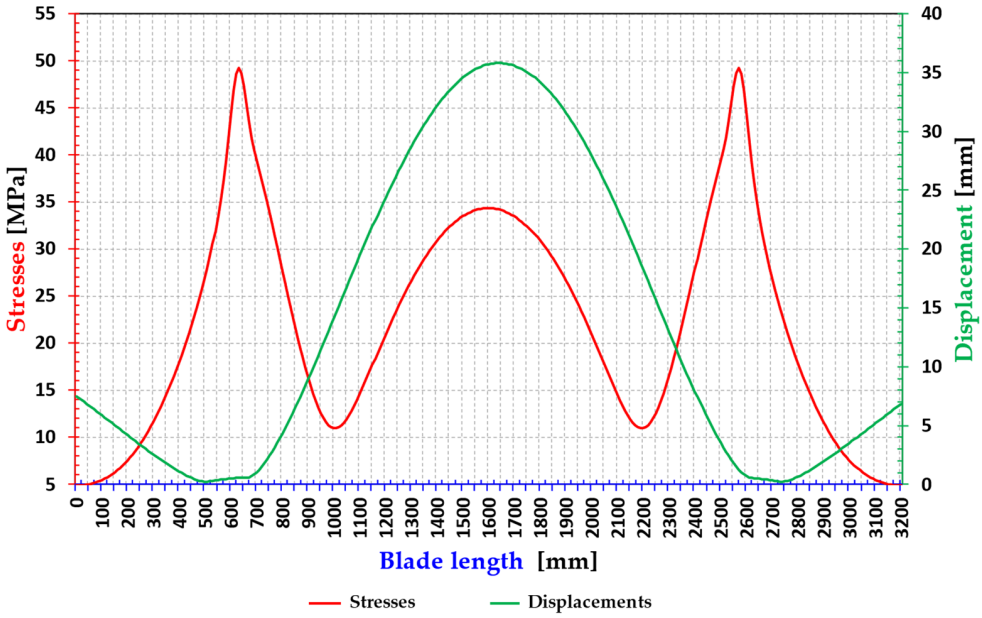

Figure 23. Maximum values of stresses and displacements at the point of application of maximum loads (c/4) of rotor blade 3 in V-Epoxy with the optimal thickness of 5 mm.

Table 10. Evaluation of the maximum and minimum stress values on the selected path in case of critical load.

		Rotor 1	
S	***S_{max}* (MPa)**	***S_{min}* (MPa)**	**Unidirectional Resistance (MPa)**
S_x	6.35	−1.707	1080
S_y	−0.274	−1.07	64
S_z	3.914	−13.768	-
S_{eq}	14.654	0.952	-
		Rotor 2	
S	***S_{max}* (MPa)**	***S_{min}* (MPa)**	**Unidirectional Resistance (MPa)**
S_x	−4.687	−6.154	1080
S_y	−3.431	−4.555	64
S_z	26.665	−23.224	-
S_{eq}	33.496	10.122	-
		Rotor 3	
S	***S_{max}* (MPa)**	***S_{min}* (MPa)**	**Unidirectional Resistance (MPa)**
S_x	−0.8924	−2.6029	1080
S_y	1.01719	−1.5678	64
S_z	37.5321	−35.4675	-
S_{eq}	49.2314	4.899	-

5.6. Discussion of the Results

1. In order to achieve a high strength-to-weight ratio for H-Darrieus-type floating wind turbine blades with three-stage rotors, they are modeled with a glass–epoxy composite material and different combinations of layers/ply orientations are analyzed. The appropriate combination of layers is found with an optimized number of layers in each direction and with varying thicknesses.
2. Keeping more layers in 90-degree directions reduces the value of maximum stresses and displacements because the applied load is normal to the chord and span of the blade. Therefore, more layers in the 90-degree direction carry the load.

3. The maximum values of stresses and displacements are evaluated at the location where the maximum loads are applied and compared to the unidirectional strength of the glass/epoxy.
4. The complete model of the three-stage rotor H-Darrieus floating wind turbine rotor 1 composite blade with an appropriate stacking sequence has maximum stresses of 103.8 MPa and maximum displacements of 2335 mm which are lower than these values (186.581 MPa and 3150 mm) for the same 5 mm aluminum wall thickness blade. Then, we applied this same stacking sequence for the composite blades of rotors 2 and 3 of the H-Darrieus floating wind turbines with three rotor stages.

6. Conclusions

It was found that centrifugal forces play an important role in the design of H-Darrieus vertical axis wind turbine blades. The bending stresses and displacements are not only a function of aerodynamic forces but also largely controlled by centrifugal forces. The effect of centrifugal forces acting on the blade can be further reduced by using glass–epoxy composite material instead of aluminum. This is because glass/epoxy has a lower density value than aluminum and a high strength-to-weight ratio. An appropriate combination of layers has to be found in order to reduce both the maximum deflections and the maximum stresses compared to the aluminum blade.

In the case of a Darrieus straight-blade VAWT, keeping more layers in a 90° orientation reduces the maximum displacement but increases the maximum stress. These maximum values can be reduced by selecting an appropriate number of layers in 90° orientation.

Therefore, the best VAWT blade design can be achieved by selecting a low-density high-strength material. Composite materials, with proper ply orientation, are the best choice to achieve these characteristics. These characteristics result in a high strength-to-weight ratio, which reduces the total weight of the blade and the centrifugal forces acting on it.

Author Contributions: Conceptualization, methodology, software, M.A.D.; validation, M.T.; investigation, M.R.; resources, A.A. and S.J.S.; data curation, H.L. and O.L.; writing—original draft preparation, M.A.D.; writing—review and editing, A.A. and M.T.; supervision, A.R. and O.B. All authors have read and agreed to the published version of the manuscript.

Funding: This research received no external funding.

Institutional Review Board Statement: Not applicable.

Informed Consent Statement: Not applicable.

Data Availability Statement: Not applicable.

Conflicts of Interest: The authors declare no conflict of interest.

References

1. Nachtane, M.; Tarfaoui, M.; Goda, I.; Rouway, M. A review on the technologies, design considerations and numerical models of tidal current turbines. *Renew. Energy* **2020**, *157*, 1274–1288. [CrossRef]
2. Nachtane, M.; Tarfaoui, M.; Saifaoui, D.; El Moumen, A.; Hassoon, O.H.; Benyahia, H. Evaluation of durability of composite materials applied to renewable marine energy: Case of ducted tidal turbine. *Energy Rep.* **2018**, *4*, 31–40. [CrossRef]
3. Rouway, M.; Nachtane, M.; Tarfaoui, M.; Chakhchaoui, N.; Omari, L.E.H.; Fraija, F.; Cherkaoui, O. Mechanical Properties of a Biocomposite Based on Carbon Nanotube and Graphene Nanoplatelet Reinforced Polymers: Analytical and Numerical Study. *J. Compos. Sci.* **2021**, *5*, 234. [CrossRef]
4. Nachtane, M.; Tarfaoui, M.; Sassi, S.; El Moumen, A.; Saifaoui, D. An investigation of hygrothermal aging effects on high strain rate behaviour of adhesively bonded composite joints. *Compos. Part B Eng.* **2019**, *172*, 111–120. [CrossRef]
5. Tarfaoui, M.; Nachtane, M.; Khadimallah, H.; Saifaoui, D. Simulation of Mechanical Behavior and Damage of a Large Composite Wind Turbine Blade under Critical Loads. *Appl Compos. Mater.* **2018**, *25*, 237–254. [CrossRef]
6. Lagdani, O.; Tarfaoui, M.; Nachtane, M.; Trihi, M.; Laaouidi, H. A numerical investigation of the effects of ice accretion on the aerodynamic and structural behavior of offshore wind turbine blade. *Wind Eng.* **2021**, *45*, 1433–1446. [CrossRef]
7. Shah, O.R.; Tarfaoui, M. The Identification of Structurally Sensitive Zones Subject to Failure in a Wind Turbine Blade Using Nodal Displacement Based Finite Element Sub-Modeling. *Renew. Energy* **2016**, *87*, 168–181. [CrossRef]

8. Lagdani, O.; Tarfaoui, M.; Nachtane, M.; Trihi, M.; Laaouidi, H. Modal analysis of an iced offshore composite wind turbine blade. *Wind Eng.* **2021**, *46*, 134–149. [CrossRef]
9. IEC IEC 61400-1:2019 IEC Webstore. Rural Electrification, Wind Power. Available online: https://webstore.iec.ch/publication/26423 (accessed on 19 March 2022).
10. Fanucci, J.B.; Walter, R.E. Innovative Wind Machines: The Theoretical Performance of a Vertical-Axis Wind Turbine. In Proceedings of the Vertical-Axis Wind Turbine Technology Workshop, Albuquerque, NM, USA, 17 May 1976; Volume 3, pp. 61–95.
11. Miliket, T.A.; Ageze, M.B.; Tigabu, M.T. Aerodynamic Performance Enhancement and Computational Methods for H-Darrieus Vertical Axis Wind Turbines: Review. *Int. J. Green Energy* **2022**, 1–38. [CrossRef]
12. Hand, B.; Kelly, G.; Cashman, A. Structural Analysis of an Offshore Vertical Axis Wind Turbine Composite Blade Experiencing an Extreme Wind Load. *Mar. Struct.* **2021**, *75*, 102858. [CrossRef]
13. Rahman, M.; Whyte, O.; Ilie, M.; Soloiu, V.; Molina, G. Structural and Aerodynamic Characteristics Analysis of a Small V-Shaped Vertical Axis Wind Turbine Rotor. *Int. J. Green Energy* **2022**, *19*, 279–299. [CrossRef]
14. Elhenawy, Y.; Fouad, Y.; Marouani, H.; Bassyouni, M. Performance Analysis of Reinforced Epoxy Functionalized Carbon Nanotubes Composites for Vertical Axis Wind Turbine Blade. *Polymers* **2021**, *13*, 422. [CrossRef] [PubMed]
15. Tarfaoui, M.; Shah, O.R.; Nachtane, M. Design and optimization of composite offshore wind turbine blades. *J. Energy Resour. Technol.* **2019**, *141*, 051204. [CrossRef]
16. Tarfaoui, M.; Khadimallah, H.; Imad, A.; Pradillon, J.Y. Design and Finite Element Modal Analysis of 48m Composite Wind Turbine Blade. *Appl. Mech. Mater.* **2012**, *146*, 170–184.
17. Tarfaoui, M.; Nachtane, M.; Boudounit, H. Finite Element Analysis of Composite Offshore Wind Turbine Blades Under Operating Conditions. *J. Therm. Sci. Eng. Appl* **2020**, *12*, 011001. [CrossRef]
18. Li, B.Y.; Karri, N.; Wang, Q. Three-dimensional numerical analysis on blade response of a vertical-axis tidal current turbine under operational conditions. *J. Renew. Sustain. Energy* **2014**, *6*, 043123. [CrossRef]
19. Marsh, P.; Ranmuthugala, D.; Penesis, I.; Thomas, G. Numerical simulation of the loading characteristics of straight and helical-bladed vertical axis tidal turbines. *Renew. Energy* **2016**, *94*, 418–428. [CrossRef]
20. Sutherland, H.J.; Berg, D.E.; Ashwill, T.D. A retrospective of VAWT technology; SAND2012-0304. In *Technical Report Sandia National Laboratories*; Sandia National Laboratories: Albuquerque, NM, USA; Livermore, CA, USA, 2012.
21. Van Den Avyle, J.A.; Sutherland, H.J. Fatigue characterization of a VAWT blade material. In Proceedings of the Eighth ASME Wind Energy Symposium, Houston, TX, USA, 22–25 January 1989; Volume 7, pp. 125–129.
22. Berg, D.E. *Structural Design of the Sandia 34-Meter Vertical-Axis Wind Turbine*; Technical Report; Sandia National Laboratories: Albuquerque, NM, USA, 1985.
23. Dabachi, M.A.; Rahmouni, A.; Bouksour, O. Design and Aerodynamic Performance of New Floating H-Darrieus Vertical Axis Wind Turbines. *Mater. Today Proc.* **2020**, *30*, 899–904. [CrossRef]
24. Dabachi, M.A.; Rahmouni, A.; Rusu, E.; Bouksour, O. Aerodynamic Simulations for Floating Darrieus-Type Wind Turbines with Three-Stage Rotors. *Inventions* **2020**, *5*, 18. [CrossRef]
25. Nachtane, M.; Tarfaoui, M.; El Moumen, A.; Saifaoui, D. Damage prediction of horizontal axis marine current turbines under hydrodynamic, hydrostatic and impacts loads. *Compos. Struct.* **2017**, *170*, 146–157. [CrossRef]
26. Lagdani, O.; Tarfaoui, M.; Rouway, M.; Laaouidi, H.; Sbai, S.J.; Dabachi, M.A.; Aamir, A.; Nachtane, M. Influence of Moisture Diffusion on the Dynamic Compressive Behavior of Glass/Polyester Composite Joints for Marine Engineering Applications. *J. Compos. Sci.* **2022**, *6*, 94. [CrossRef]
27. Hameed, M.S.; Afaq, S.K. Design and Analysis of a Straight Bladed Vertical Axis Wind Turbine Blade Using Analytical and Numerical Techniques. *Ocean Eng.* **2013**, *57*, 248–255. [CrossRef]
28. Three-Dimensional Solid Element Library. Available online: https://abaqus-docs.mit.edu/2017/English/SIMACAEELMRefMap/simaelm-r-3delem.htm (accessed on 19 March 2022).
29. Anderson, J.D., Jr. *Fundamentals of Aerodynamics*; Tata McGraw-Hill Education: New York, NY, USA, 2010.
30. Emami, M.R. *Aerodynamic Forces on an Airfoil*; AER 303F; Aerospace Laboratory I University of Toronto: Toronto, ON, Canada, 2007.
31. Batz—Burgel. Al EN AW-2017A (AlCu4MgSi—3.1325) Aluminium. Available online: https://batz-burgel.com/en/metal-trading/aluminium-product-range/en-aw-2017a/ (accessed on 3 March 2022).
32. Islam, M.; Fartaj, A.; Carriveau, R. Analysis of the Design Parameters Related to a Fixed-Pitch Straight-Bladed Vertical Axis Wind Turbine. *Wind Eng.* **2008**, *32*, 491–507. [CrossRef]
33. Sutherland, H.J. A Summary of the Fatigue Properties of Wind Turbine Materials. *Wind Energy Int. J. Prog. Appl. Wind Power Convers. Technol.* **2000**, *3*, 1–34. [CrossRef]
34. Wang, L.; Kolios, A.; Nishino, T.; Delafin, P.-L.; Bird, T. Structural Optimisation of Vertical-Axis Wind Turbine Composite Blades Based on Finite Element Analysis and Genetic Algorithm. *Compos. Struct.* **2016**, *153*, 123–138. [CrossRef]
35. Barnes, R.H.; Morozov, E.V. Structural Optimisation of Composite Wind Turbine Blade Structures with Variations of Internal Geometry Configuration. *Compos. Struct.* **2016**, *152*, 158–167. [CrossRef]
36. Gay, D.; Hoa, S.V.; Tsai, S.W. *Composite Materials: Design and Applications*; CRC Press: Boca Raton, FL, USA, 2002; ISBN 978-0-429-13496-8.
37. Navadeh, N.; Goroshko, I.; Zhuk, Y.; Etminan Moghadam, F.; Soleiman Fallah, A. Finite Element Analysis of Wind Turbine Blade Vibrations. *Vibration* **2021**, *4*, 310–322. [CrossRef]

38. Hameed, M.S.; Afaq, S.K.; Shahid, F. Finite Element Analysis of a Composite VAWT Blade. *Ocean Eng.* **2015**, *109*, 669–676. [CrossRef]
39. El Moumen, A.; Tarfaoui, M.; Hassoon, O.; Lafdi, K.; Benyahia, H.; Nachtane, M. Experimental study and numerical modelling of low velocity impact on laminated composite reinforced with thin film made of carbon nanotubes. *Appl. Compos. Mater.* **2018**, *25*, 309–320. [CrossRef]